17th World Conference on Earthquake Engineering, 17WCEE
Sendai, Japan - September 13th to 18th 2020

FEASIBILITY STUDY ON EARTHQUAKE EARLY WARNING SYSTEM FOR THE CITY OF LIMA, PERU, USING A STRONG-MOTION NETWORK

Cinthia Calderon[(1)], Takumi Hayashida[(2)]

[(1)] *Research Assistant Associate, Peru, Japan Peru Center for Earthquake Engineering Research and Disaster Mitigation (CISMID), cinthia.calderon.c@uni.pe*
[(2)] *Senior Research Scientist, International Institute of Seismology and Earthquake Engineering (IISEE) Building Research Institute, Japan, takumi-h@kenken.go.jp*

Abstract

Feasibility of earthquake early warning system (EWS) for the city of Lima, Peru, was investigated using strong motion records data from the newly installed real-time strong motion observation network of the Japan Peru Center of Seismic Investigation and Disaster Mitigation (CISMID). The operation of the network started in 1988. We selected earthquakes occurred in 2017, the operation of the network obtained 347 records from 24 events. The magnitudes of the events are bigger than or equal to ML 3.5 and the focal depths are smaller or equal to 100 km. There were 19 observation stations in Lima with 2-12 km station intervals. At each station strong-motion accelerograph REFTEK 130-SMA is installed at sample frequency of 200 Hz. The sizes and locations of the selected events were estimated using the initial P-wave portions (3 seconds) of the observed waveforms, based on the conventional approaches. For the estimation of the magnitude, we determined the "tauc" parameter that relates to earthquake magnitude. We found a reasonable correlation between the estimated magnitudes and the catalogue magnitudes for shallower and relatively larger earthquakes in the vicinity (distance < 130 km). The hypocenter locations were determined with the detected P-wave arrival times. Since the observation stations are distributed only in the limited area of Lima, we found that the hypocenters are not well determined and we need at least eight stations to stably estimate the locations. To investigate the accuracy of the existing ground-motion prediction equations (GMPEs) in the real-time scheme, we selected two GMPEs for subduction zone earthquakes to compare the predicted peak ground accelerations (PGA) with the observed ones. In most cases the GMPEs tend to overestimate PGAs, possibly due to large site amplification in Lima. It could be also another reason that these GMPEs were developed for other environments using only larger earthquakes. The blind zone is defined as the region around the epicenter where no warning is issued because the strong shaking has already arrived by the time the alert is generated (Kuyuk and Allen, 2013). We also confirmed that the size of blind zones of the earthquake early warning system is not so large for most earthquakes and it is possible to give an alert to the city of Lima before S-wave arrivals, if the hypocenter locations (i.e. distance from the hypocenter) were correctly determined.

Keywords: Earthquake Early Warning, Lima, P-waves, Peak ground acceleration, Blind zone.

1. Introduction

Peru is located in the most seismically active region of the world, called the Circum-Pacific belt or Pacific Ring of Fire. Lima City, the capital of Peru, experienced earthquakes and tsunamis frequently due to the location (Fig. 1). The last large event in the city occurred in 1974 (Mw 8.0) and strong ground motions hit the coastal areas of Lima and Callao, causing severe damage. More than 40 years have passed since then and the probability of larger seismic events has been increasing. According to earthquake scenarios by Pulido et al. (2015), an Mw 8.9 earthquake in the central coast of Peru would directly affect Lima City is expected to occur. Earthquakes EWS can be used to prepare the citizens for the earthquake just before the strong ground shakings and reduce the casualty and economic loss. The purpose of this study is to examine the performance and expected problems of an earthquake EWS in Peru using data from the newly installed real-time strong ground motion network.

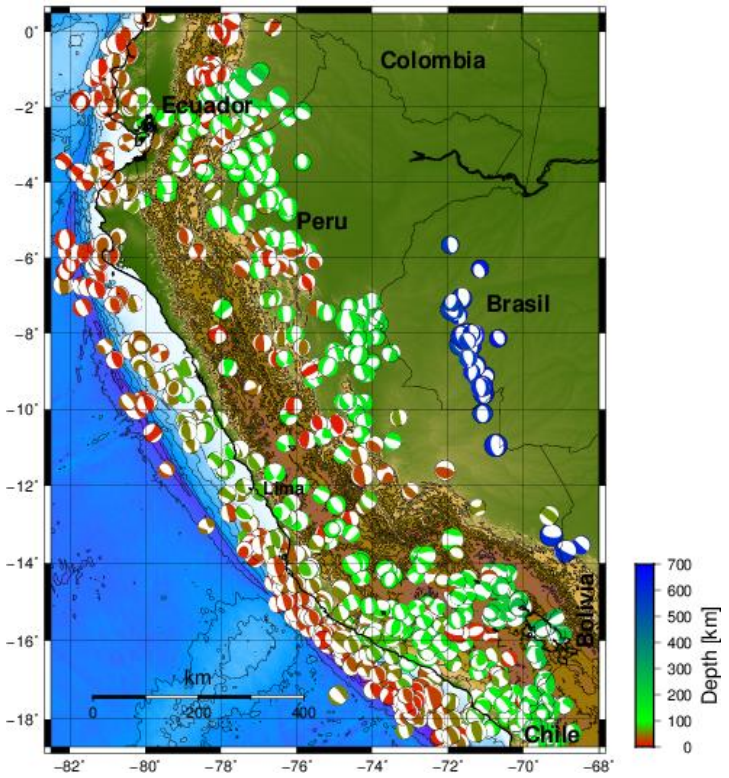

Fig. 1 – Map showing seismic activity in Peru from 1976 to 2018, for earthquakes of magnitude ≥ 5 (earthquake data from USGS; focal mechanisms from CMT catalog).

2. Data

The data presented in this study was taken from the accelerograph network that belongs to the Japan Peru Center for Earthquake Engineering and Disaster Mitigation (CISMID). At each station strong-motion accelerograph REFTEK 130-SMA is installed at sample frequency of 200 Hz. There are 19 observation stations in Lima with 2-12 km station intervals. We selected earthquakes occurred in 2017 when the operation of the network started and obtained 347 records from 24 events. The magnitudes of the events are bigger than or equal to ML 3.5 and the focal depths are smaller or equal to 100 km. Table 1 is the list of the events used in this study.

Table 1 – Catalog of the selected data after the magnitude estimation (data from the accelerograph network of CISMID).

Origin Time (UT)	Lat.	Lon.	Depth (Km)	Magnitude (ML)	No. Records	No. Select. Records
2017/5/3 19:05:49	-12.24°	-77.40°	32	4.0	9	9
2017/5/11 10:32:47	-12.07°	-77.45°	31	3.9	8	8
2017/7/8 20:07:24	-11.72°	-77.37°	73	4.8	12	12
2017/9/14 8:19:23	-11.91°	-76.34°	40	4.8	17	17
2017/9/15 4:10:36	-11.91°	-76.33°	18	4.4	16	5
2017/9/25 19:54:14	-11.96°	-77.66°	28	4.0	17	3
2017/10/22 0:09:13	-12.32°	-77.34°	36	4.7	17	17
2017/11/1 3:36:03	-11.77°	-77.55°	50	4.4	19	16
2017/11/24 2:24:26	-12.10°	-77.55°	46	4.1	19	12
2017/11/24 11:15:53	-12.09°	-76.25°	76	4.7	19	17

3. Methodology

3.1 Tauc (τc) parameter

In order to determine the size of an earthquake, it is important to know if the fault rupture stopped or is still growing, which is generally reflected in the period of the initial motion (Wu and Kanamori, 2005). We use an average of the period during the first motion (3 s of initial P-wave) to judge the source process. At first, we computed the ratios of displacement $u(t)$ and the velocity $\dot{u}(t)$ waveforms using the vertical component of initial P-wave motions with the relation showed in ecuation (1)

$$r = \frac{\int_0^{\tau_0} \dot{u}^2(t)dt}{\int_0^{\tau_0} u^2(t)dt}. \quad (1)$$

The integration is over the time (0, τ0) after the P-wave onset. We assigned 3 s for τ0. According to Parseval's theorem, Eqs. (1) can be modified as Eqs. (2):

$$r = \frac{4\pi^2 \int_0^{\infty} f^2 |\hat{u}(f)|^2 df}{\int_0^{\infty} |\hat{u}(f)|^2 df} = 4\pi^2 \langle f^2 \rangle , \quad (2)$$

where $|\hat{u}(f)|$ is the amplitude spectra of $u(t)$ and $\langle f^2 \rangle$ is the average of f^2 weighted by $|\hat{u}(f)|^2$.Finally, the parameter τ_c is defined as Eqs. (3):

$$\tau_c = \frac{1}{\sqrt{\langle f^2 \rangle}} = \frac{2\pi}{\sqrt{r}}, \tag{3}$$

and the relationship between the average τ_c and magnitude is formulated (Kanamori, 2005; Wu and Kanamori, 2005) as Eqs. (4):

$$M_{est}(\tau_c) = (4.525)\log \tau_c + 5.036 \tag{4}$$

3.2 Automatic Picking of P-wave

To detect the initial arrival of P wave automatically from the observed waveforms, we tested the automatic phase-picking algorithm proposed by Allen (1982). The detection of the event is accomplished by comparing a characteristic function or its short-term average (STA) with a threshold value (THR). If the STA exceeds THR, a trigger (P arrival) is declared.

3.3 Automatic Picking of P-wave

In Peru, there is no original ground motion prediction equation (GMPE) and various existing GMPEs derived in other seismotectonic environments have been tested. The frequently used ones are the attenuation law of Youngs et al. (1997) and Zhao et al. (2006).

3.3.1 Ground Motion Prediction Equation of Youngs et al. (1997)

The relationship was developed based on regression analyses using data from 174 earthquakes in Alaska, Chile, Cascadia, Japan, Mexico, Peru, and Salomon Islands. They used events whose moment magnitude was larger than or equal to 5 and hypocentral distance from 10 to 500 km. There are two different functional forms of the relationship depending on site characteristics (soil site and rock site). Here we assumed that rupture distance is equivalent to hypocentral distance and source types of all earthquakes are interplate events.

For soil site (Eq. (5)) and for rock site (Eq. (6)). Ground motion model for soil is

$$\ln PGA = C_1^* + C_2 M + C_3^* \ln\left| r_{rup} + e^{C_4^* - \frac{C_2}{C_3^*}M} \right| + C_5 Z_t + C_9 H + C_{10} Z_{ss}, \tag{5}$$

where $C_1^* = C_1 + C_6 Z_r, \quad C_3^* = C_3 + C_7 Z_r, \quad C_4^* = C_4 + C_8 Z_r.$

Here unit of PGA is given in g, and the other coefficients are C1=-0.6687, C2=1.438, C3=-2.329, C4=ln(1.097), C5=0.3643, C9=0.00648, M: magnitude in Mw, rrup: rupture distance in km (hypocenter distance can be used for small earthquake), Zss: indicates shallow stiff (1 for shallow soil sites and 0 for otherwise), H: focal depth in km and σ=1.45 – 0.1M, respectively.

For rock site, the equation is

$$\ln PGA = C_1^* + C_2 M + C_3^* \ln\left| r_{rup} + e^{C_4^* - \frac{C_2}{C_3^*}M} \right| + C_5 Z_{ss} + C_8 Z_t + C_9 H \tag{6}$$

where $C_1^* = C_1 + C_3 C_4 - C_3^* C_4^*, \quad C_3^* = C_3 + C_6 Z_{ss}, \quad C_4^* = C_4 + C_7 Z_{ss}.$

Here the coefficients are C1=0.2418, C2=1.414, C3=-2.552, C4=ln(1.7818), C8=0.3846, C9=0.00607, M: magnitude in Mw, rrup: rupture distance in km (hypocenter distance can be used for small earthquake),

Zt: indicates source type (0 for interface events and 1 for intraslab events), Zss: indicates shallow stiff (1 for shallow soil sites and 0 for otherwise), H: focal depth in km and σ=1.45 – 0.1M, respectively.

3.3.2 Ground Motion Prediction Equation of Zhao et al. (2006)

The authors used 4518 earthquakes in Japan, 208 earthquakes in Iran and Western USA. In the dataset the maximum focal depth is 162 km and the maximum source distance is 300 km. The events are classified into three source types; crustal, interplate and intraslab earthquakes. The maximum possible values for source depth is 25 km for crustal events, 50 km for interface events, and between 15 and 162 km for intraslab events. This equation (7) also considers site conditions and the site amplification is evaluated depending on the NEHRP (National Earthquake Hazards Reduction Program) site classification.

The ground motion model is expressed as;

$$\log_e(y) = aM_w + bx - \log_e(r) + e(h - h_c)\delta_h + F_R + S_I + S_S + S_{SL}\log_e(x) + C_k, \quad (7)$$

where h: focal depth in km, hc: depth constant , Mw: moment magnitude, x: source distance in km, $r = x + c\exp(dM_w)$ .The parameter y corresponds to PGA (cm/s2), δh=1 when h ≥ hc and 0 otherwise, a=1.101, b=-0.00564 c=0.0055, d=1.080, e=0.01412 SR=0.251, SI=0.000, SS=2.607, SSL=-0.528, CH=0.293, C1=1.111, C2=1.344, C3=1.355, C4=1.420, σ=0.604 (intra-event) and τ=0.398 (inter-event).

In this equation five different site classes are considered, by changing parameters C. Here CH, C1, C2, C3, and C4 are used for hard rock site (NERHRP site class A, Vs,30 > 1100 m/s), rock site (NERHRP site classes A+B, 600 < Vs,30 ≤ 1100 m/s), hard soil site (300 < Vs,30 ≤ 600 m/s), medium soil site (200 < Vs,30 ≤ 300 m/s), and soft soil site (Vs,30 ≤ 200 m/s), respectively. T is natural frequency of soil and VS30 is averaged S-wave velocity in the top 30 m.

3.4 Tauc (τc) parameter

In the analysis of GMPEs in this study we used information of hypocenter location and event magnitude from CISMID catalogue. However, the above two formulas use moment magnitude for magnitude parameter, while local magnitude is determined in the catalogue. Cahuari (2008) proposed relationships between ML, mb, Ms, and Mw using the data of Peru in Equation (8). She used 112 earthquakes in Peru during the period of 1990-2015 to derive the relationships. These earthquakes are located in the south area of Peru and in less quantity in the central and north area of Peru, however, the database is homogeneous. The relationship between ML and MW was expressed with a simple linear relationship.

$$Mw = 0.9879ML + 0.3316 \quad (8)$$

3.5 Data preprocessing

As stated above we selected 24 earthquakes and downloaded all the records from the website of the Seismic Monitoring Center (CEMOS) of CISMID showing in Figure 11. The original records were in the ascii format (.txt), which contains header information (observation time, station ID and location and sampling frequency) and a series of acceleration amplitudes in the three components; NS, EW and UD, respectively.

Initially, we converted the original data, from text format files (.txt) to the SAC format files, using the computer program provided by Dr. Takumi Hayashida "txt2sac", since the software in the following steps require the waveform data in SAC format.

Then, we checked all the waveform data before processing and noticed that some of them presented noise, because the source-to-sensor distances were very long (several hundred km), hypocenters were deep, or magnitude scales were small. Therefore, in order to recognize the first P-trigger arrival and to do not affect the "τc" parameter, we applied a 20 Hz low pass filter type in advance.

4. Methodology

4.1 Magnitude estimation

The magnitude was computed using the software "tauc" provided by Dr. Masumi Yamada, which is based on the Tauc (τc) theory. We applied the software "tauc" for all the stations and events, considering two parameters, 0.2 Hz for the cutoff frequency of Butterworth high pass filter and 0.05 gal for acceleration threshold value.

After the processing for all the recordings (as is shown in Figure 2), we selected the data again because the estimated values of magnitude were largely overestimated for events whose epicentral distance was long and whose magnitude was small, due to low S/N ratios. After the screening, we found that the software can be applied to data whose hypocentral distance is less than 130 km and magnitude is larger than 3.5. The number of available events was reduced to 10, although the predicted magnitude scales are slightly overestimated.

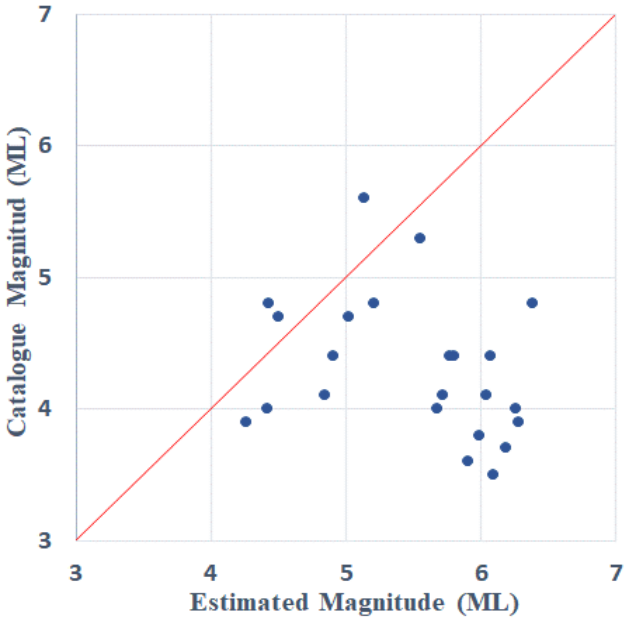

Fig. 2 – Comparison between the catalogued and estimated magnitude for the selected 24 events.

4.2 Hypocenter location estimation

The hypocenter estimation was computed with the software "hypo" developed by Dr. Takumi Hayashida, which uses the automatically picked P-wave arrivals to find reasonable hypocenter location that reduces the detected and predicted P-wave arrivals by repeated calculation. In general, the results show large differences between estimated and catalogue hypocenter locations as is shown in Figure 3, which were not reasonable due to the lack of stations along the coastal line for the case of subductions earthquakes.

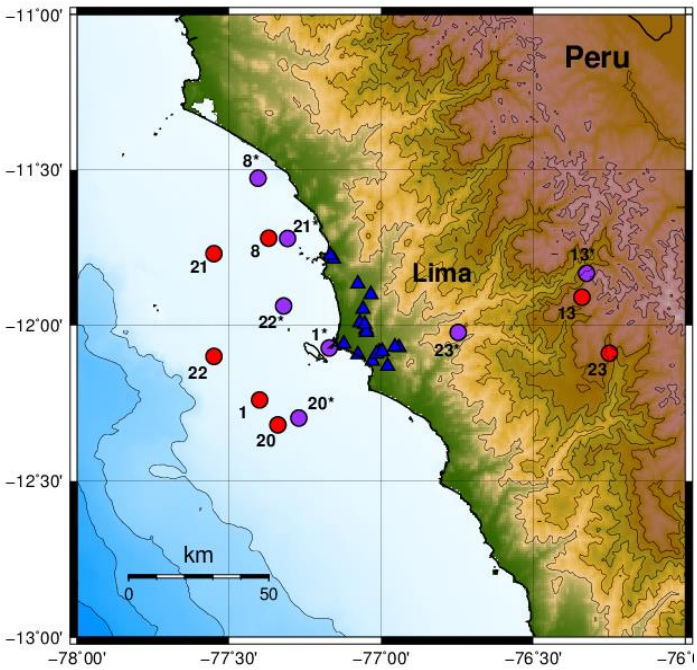

Fig. 3 – Map showing epicentral locations of the selected events (red circles: catalogue epicenters, purple circles: estimated epicenters).

4.3 Peak Ground Acceleration estimation

We obtained the observed PGAs from the dataset. We also applied the two GMPEs, considering soil conditions (Vs30 values) where the stations are located. We found that the agreement overestimated, underestimated and good correlations on the calculated values of PGA as is shown in Figure 4.

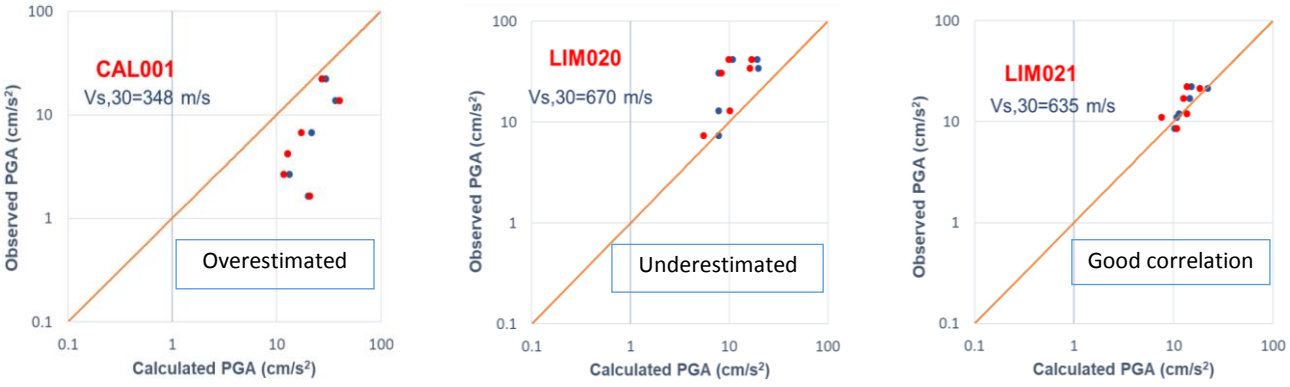

Fig. 4 – Comparison between the observed and predicted PGAs at three stations.

4.4 Analysis of the blind zone

Earthquake Early Warning Systems usually has a blind zone around the epicenter where the S-wave arrives ahead of or coincident with the warning issuance. The blind zone is defined as the region around the epicenter where no warning is issued because the strong shaking has already arrived by the time the alert is generated (Kuyuk and Allen, 2013).

Figure 5 shows the result of blind zone analysis for an event (date, time, magnitude, depth). Here we assumed that 3 seconds is required for the processing. For this earthquake P-wave front reached the farthest station 11.9 s after the earthquake origin time and we found that at least 14.9 s is needed to determine magnitude and hypocenter location, and give a first alert to Lima (dashed black line). According to this result, the S-wave front arrives at a distance of 38.5 km at the warning time and Lima is outside of the blind zone. However, the result with the real-time estimated epicenter location indicates that the S-wave reaches all the stations at the warning time and this differs from the actual observations. This indicates that the estimated hypocenter is not reliable and accurate estimation of hypocentral location is important to prevent false alert and to find the affected area.

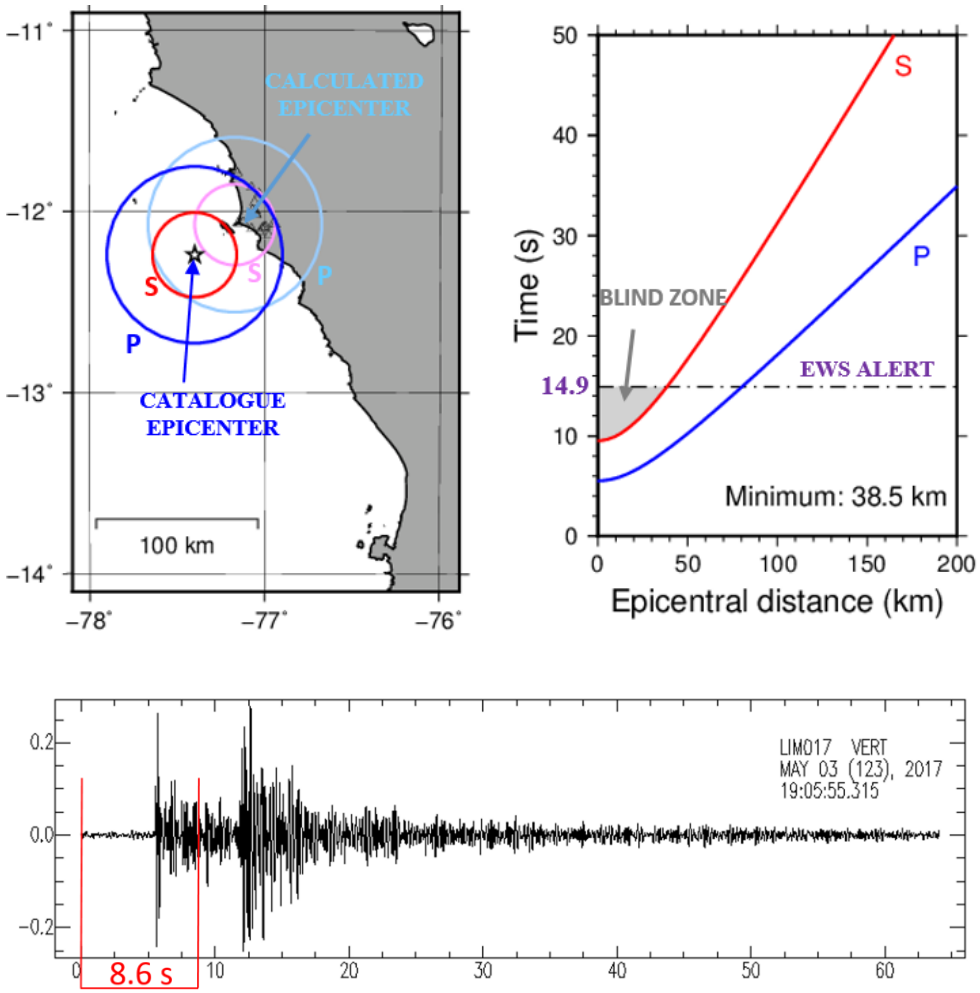

Fig. 5 – Left: Map of the calculated and catalogue (star) epicenter locations, along with P- and S-wave arrivals. Right: Time-distance plot illustrating the relative timing of arrivals of P and S waves, warning time and blind zone. On the bottom, the waveform of the last station recording the earthquake shows the acceleration when the warming is emitted (8.6 s since the recording of the station).

4.5 Experiment on determination of the epicentral distance using single stations

In this study, we also investigated the possibility to estimate epicentral locations using a single-station approach, since we have difficulty in accurate estimations of hypocenter location. Odaka et al. (2003) proposed a concept of estimation of epicentral distance and this is based on the analysis of the initial P-wave portion (2-3 s) observed at a single seismic station. In this method, the coefficient B is treated as an index to indicate the increasing ratio (i.e. slope of the envelope) of the P-wave. It can be obtained by fitting the envelope curve of absolute amplitude for the observed P-wave's initial phase into the following equation (9);

$$y(t) = Bt\exp(-At) \quad , \tag{9}$$

where y represents envelope of high-frequency UD-component acceleration and t represents the time after P-wave onset. Parameter A is the regression coefficient that relates to earthquake size. After that, Yamamoto et al. (2012) proposed a method to improve the performance of the approach using the following approximation Eq. (10),

$$y(t) = Ct \quad , \tag{10}$$

where coefficients C are derived by an ordinary least square regression. This method utilizes only 0.5 s window data of P-wave initial motion.

Here we tested the C-Δ method in this study to investigate if it can be a reasonable tool for the estimation of the epicentral distance also in Peru. For the procedure, we considered a 10-20 Hz bandpass filter and extracted 0.5 s of the P-wave onset for all earthquake recordings selected in this study. The relationship between the derived C value and the epicenter distance is shown in Figure 6. The number of data is limited and it is difficult to establish a reliable formula in Peru, but the derived trend is similar to those of Japan (Yamamoto et al., 2012).

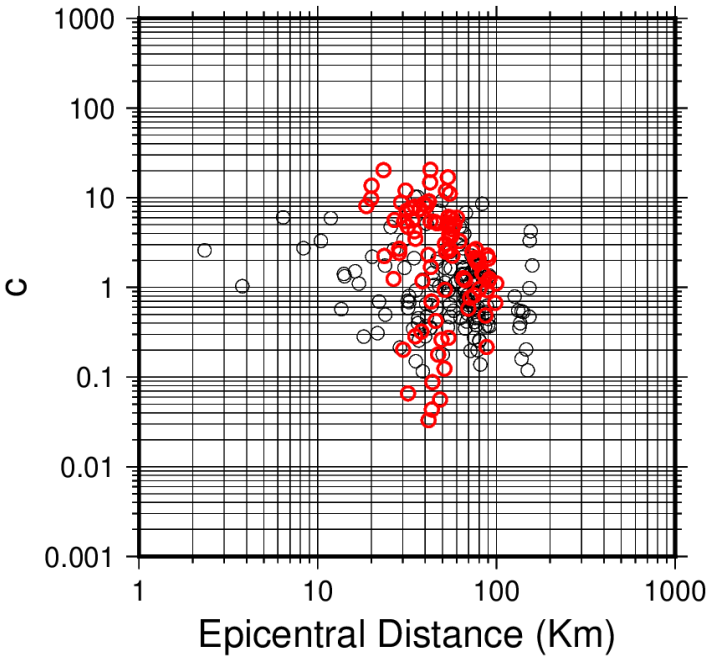

Fig. 6 –Relationship between C values and epicentral distance Δ for earthquakes presented in this study. Black circles represent the total data (24 earthquakes) and red circles represent the selected data (10 earthquakes).

5. Conclusions

In the hypocenter determination, we found that at least 8 stations are needed to estimate the hypocentral parameters. When the number of the seismic stations was larger than 16, the results were good and the hypocenter locations became very similar to those of the CISMID catalogue. On the other hand, when the number of the stations was between 9 and 12, the results were not reasonable, indicating that real-time observation stations should be distributed not only in Lima city, but also outside the city.

From the PGAs comparison, we noticed an overestimated tendency in the calculated values of PGA for stations with small Vs30 values (≤ 500 m/s). On the other hand, we also noticed an underestimated tendency in the calculated values of PGA for those stations with larger Vs30 values.

We found that the blind zone cannot be a big problem in the case of Lima but it is not feasible to install EWS in Peru at the present, because the hypocentral locations were not well determined under the present observation network.

Moreover, the determination of epicentral distance using single station can be used for the case of Peru, since we do not have enough seismic stations and it is used also for small earthquakes. We found a relationship between the C parameter and the epicentral distance of the earthquakes used for this study, and this information could help to implement the earthquake EWS of Peru in the future.

6. Recommendation

For the reasonable detection of subduction zone earthquakes, the stations should be located along the coastal line.

It is important to remember that the values of PGAs were calculated with GMPEs from other countries. Therefore, in order to increase the accuracy of the predictions the development of GMPE in the study area is recommended.

In order to increase the accuracy of the source-to-station distance, further accumulation of earthquake data including future earthquakes and past earthquakes are needed.

7. Acknowledgements

I would like to express my gratitude to my supervisor Dr. Takumi Hayashida and Dr. Toshiaki Yokoi for their guidance, teachings, kindness, valuable suggestion and instruction during my study.

8. References

[1] ALLEN, R., 1982, BULL. SEISM. SOC. AM., 72, 6B, S225-S242.

[2] CAHUARI A., 2008, " CÁLCULO DE LA MAGNITUD LOCAL (ML) A PARTIR DE REGISTROS DE ACELERACIÓN USANDO LA TÉCNICA DECONVOLUCIÓN Y RELACIÓN DE MAGNITUDES", (IN SPANISH), THESIS OF DEGREE, FACULTY OF GEOLOGY, GEOPHYSICS AND MINES, SAN AGUSTIN NATIONAL UNIVERSITY OF AREQUIPA, AREQUIPA, PERU.

[3] KANAMORI, H., 2005, ANNU. REV., EARTH PLANET. SCI., 33, 195-214.

[4] KENNETT, B. L. N., ENGDAHL, E. R., 1991, GEOPHYSICAL JOURNAL INTERNATIONAL, 105, 2, 429-465.

[5] KUYUK, H. S., ALLEN, R. M., 2013, SEISMOLOGICAL RESEARCH LETTERS, 84, 6, 946-954.

[6] NAKAMURA, Y., 1988, IN PROC. OF THE 9TH WORLD CONFERENCE ON EARTHQUAKE ENGINEERING, 7, 673-678.

[7] ODAKA, T., ASHIYA, K., TSUKADA, S. Y., SATO, S., OHTAKE, K., NOZAKA, D., 2003, BULL. SEISM. SOC. AM., 93, 1, 526-532.

[8] PULIDO, N., AGUILAR, Z., TAVERA, H., CHLIEH, M., CALDERÓN, D., SEKIGUCHI, T., YAMAZAKI, F., 2015, BULL. SEISM. SOC. AM., 105, 1, 368-386.

[9] WU, Y. M., KANAMORI, H., 2005, BULL. SEISM. SOC. AM., 95, 1, 347-353.

[10] YAMAMOTO, S., NODA, S., KORENAGA, M., 2012, RTRI REPORT, 26, 9, 5-10.

[11] YOUNGS, R. R., CHIOU, S. J., SILVA, W. J., AND HUMPHREY, J. R., 1997, SEISM. RES. LETTERS, 68, 1, 58-73.

[12] ZHAO, J. X., ZHANG, J., ASANO, A., OHNO, Y., OOUCHI, T., TAKAHASHI, T., OGAWA, H., IRIKURA, K., THIO, H., K., SOMERVILLE, P., FUKUSHIMA, Y., 2006, BULL. SEISM. SOC. AM., 96, 3, 898-913.

